NanoImpact 41 (2026) 100608

Contents lists available at ScienceDirect

NanoImpact

journal homepage: www.elsevier.com/locate/nanoimpact

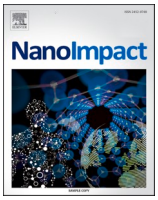

Impact of titanium dioxide and cerium dioxide nanoparticle mixtures on the green alga *Raphidocelis subcapitata*

Mariam Bakir [a], Isabel Abad-Alvaro [b], Francisco Laborda [b], Vera I. Slaveykova [a,*]

[a] Environmental Biogeochemistry and Ecotoxicology, Department F.-A. Forel for Environmental and Aquatic Sciences, Faculty of Sciences, University of Geneva, 66 Blvd Carl-Vogt, CH 1211 Geneva, Switzerland
[b] Group of Analytical Spectroscopy and Sensors (GEAS), Institute of Environmental Sciences (IUCA), University of Zaragoza, Pedro Cerbuna, 12, 50009 Zaragoza, Spain

ARTICLE INFO

Keywords:
Green algae
Cocktail effects
Nanomaterials
Oxidative stress
Antagonistic interaction
Mixtures

ABSTRACT

Engineered nanoparticles (NPs) occur as mixtures in the environment, making the study of their combined toxicity more realistic than the assessment of individual NPs. Interactions between NPs can alter toxicity profiles, producing synergistic, antagonistic, or additive effects, yet current environmental assessments often overlook these cocktail effects. This study investigated the effects of titanium dioxide NPs (TiO_2-NPs) and cerium dioxide NPs (CeO_2-NPs) mixtures on the green alga *Raphidocelis subcapitata* compared individual NP exposures. Four mixtures with varying NP ratios were designed based on the toxicity units (TUs) concept and EC_{50} growth-inhibition values for TiO_2-NPs of 28.3 ± 1.16 mg L^{-1}, and EC_{50} for CeO_2-NPs of 13.6 ± 0.57 mg L^{-1}. Growth inhibition, reactive oxygen species (ROS) generation, and membrane damage were assessed using flow cytometry (FCM), while uptake was analyzed by single-cell inductively coupled plasma mass spectrometry (SC-ICP-MS). Single-particle (SP) -ICP-MS distinguished NP size distribution and dissolution in mixtures.

Results revealed antagonistic interactions in mixtures, with growth inhibition lower than expected based on individual treatments. The difference between predicted and measured TUs in the mixture treatments, used as a measure for the extent of antagonistic interaction ranged from 0.66 to 1.76. Cells with elevated ROS generation showed a two- to four-fold reduction in the mixtures versus single NP treatments. SC-ICP-MS indicated reduced bioavailability of NPs in mixtures: intracellular TiO_2-NP content decreased from 15.7 to 24.3 fg $cell^{-1}$ (single) to 12.9–15.9 fg $cell^{-1}$ (mixture), and CeO_2-NP content dropped from 3.6 to 8.6 fg $cell^{-1}$ to 2.7–3.8 fg $cell^{-1}$. This study demonstrates the importance of assessing NP mixture toxicity using advanced single-event techniques, such as FCM, SP- and SC-ICP-MS, to discriminate the fate and bioavailability of NPs present in mixtures and to better understand their environmental impacts.

1. Introduction

Aquatic organisms are typically exposed to complex mixtures of environmental pollutants, including engineered nanoparticles (NPs) (Li et al., 2020; Zhang et al., 2022). Assessing the combined effects of multiple NPs and predicting the toxicity of NPs mixtures are essential for a more realistic evaluation of their ecological risks (Keller and Slaveykova, 2025). Indeed, the co-existence of different types of NPs in aquatic environment can lead to a variety of interactions - antagonistic, synergistic, or additive - resulting in effects that differ from those observed with individual NP exposure (Li et al., 2020; Martinez et al., 2022; Wang et al., 2024b). A review of 86 studies on the ecotoxicity of NPs mixtures found that 53 % of interactions were antagonistic, 25 % were synergistic and 22 % were additive (Zhang et al., 2022). Studies have compared the effects of NPs in mixtures to single NPs, highlighting the complexity of interactions and their variable outcomes (Das et al., 2023b; Das et al., 2022; Ghariani et al., 2025; Huang et al., 2019; Huang et al., 2021; Iswarya et al., 2015; Ko et al., 2018; Liu et al., 2018; Pikula et al., 2022; Rana and Kumar, 2023a, 2023b). For instance, the combination of SiO_2-NPs and ZnS-NPs exhibited an antagonistic effect on the mixotrophic alga *Heterosigma akashiwo*, likely due to the scavenging of Zn^{2+} and interactions between ZnS-NPs and SiO_2-NPs (Pikula et al., 2022). Similarly, the interactions between SiO_2-NPs and Al_2O_3-NPs led to the formation of hetero-aggregates, which reduced their bioavailability to green alga *Chlorella vulgaris* and consequently decreased the toxicity of Al_2O_3-NPs (Huang et al., 2021). Antagonistic effects of

* Corresponding author.
E-mail address: vera.slaveykova@unige.ch (V.I. Slaveykova).

https://doi.org/10.1016/j.impact.2025.100608
Received 15 September 2025; Received in revised form 23 November 2025; Accepted 15 December 2025
Available online 16 December 2025

mixtures of ZnO-NPs and CuO-NPs to biomass of *Scenedesmus obliquus* were observed at concentrations of 1 and 10 mg L^{-1} over a 35 day period (Rana and Kumar, 2023b). Antagonistic effect was also observed when Ag-NPs were combined with hematite nanoparticles (He-NPs), as Ag^{+} was adsorbed onto He-NPs, reducing Ag bioavailability and toxicity to golden-brown microalga *Ochromonas danica* (Huang et al., 2019). Mixture of Ag-NPs and Hg exhibited an antagonistic effect on diatom *Chaetoceros muelleri* (Mosleminejad et al., 2024). Similarly, TiO_2-NPs significantly mitigated the impact of Hg^{2+} on the growth and photosynthesis of green alga *Chlamydomonas reinhardtii* (Li et al., 2020). Antagonistic interaction was also observed in another green alga *Raphidocelis subcapitata*, where exposure to SiO_2-NPs in combination with pesticides, such as paraquat, pentachlorophenol, and diflufenican, reduced toxicity (Book et al., 2022). Conversely, exposure to some NP-containing mixtures resulted in additive effects, such as the combination of TiO_2-NPs and bisphenol A on green alga *Scenedesmus obliquus* (Das and Mukherjee, 2024). On the other hand, synergistic interactions have also been reported, for example, TiO_2-NPs enhanced the toxicity of tetracycline (Roy et al., 2021). A mixture of SiO_2, Fe_3O_4 and ZnO-NPs synergistically affected the *S. obliquus* (Das et al., 2023a), as well as mixture of polystyrene NPs increased toxicity in *O. danica* and *C. reinhardtii* (Huang et al., 2019). Despite notable advancements in our understanding, as illustrated by the selected examples, a significant research gap persists in unravelling the complexity and variability of the effects of NP mixtures on aquatic biota (Zhang et al., 2022) including the long-term and sublethal effects of mixtures, species-specific responses, lack of predictive, mechanistic models (e.g., based on Toxic Units (TUs) or concentration-addition frameworks) that consider both NP–NP interactions and species variability. Gaining deeper insights into how NP mixtures interact with phytoplankton species is essential for developing effective environmental regulations and management strategies to mitigate their potential ecological impact.

In such a context, the present study aims to explore the interactions of four different mixtures of TiO_2-NPs and CeO_2-NPs on *Raphidocelis subcapitata* and compares the observed effects with treatments involving individual NPs. TiO_2-NPs and CeO_2-NPs were selected because they exhibit contrasting redox and surface properties and are among the most widely used NPs (Dar et al., 2020; Pansambal et al., 2022). TiO_2-NPs are commonly utilized in paints, personal care products and photocatalytic applications (Musial et al., 2020). CeO_2-NPs find applications in photocatalysis as well as in biological context, serving as antibacterial, antifungal, antioxidant, antidiabetic, or anticancer agents (Pansambal et al., 2022).

Raphidocelis subcapitata was chosen as a representative primary producer in freshwater ecosystems, contributing to oxygen generation, nutrient cycling, and food web support (Machado and Soares, 2024). *R. subcapitata* responds rapidly to changes in water chemistry and pollutant exposure, making it a recognized standard test organism for evaluating chemical and nanomaterial toxicity and a reliable bio-indicator of aquatic ecosystem health.

To evaluate mixture toxicity, various ratios of TiO_2-NPs and CeO_2-NPs in the mixtures were selected using the TU framework. While TU-based models are widely used in chemical ecotoxicology to quantify synergistic or antagonistic interactions (Vilela et al., 2023), they remain underused in studies of NP mixtures. Biological endpoints, such as growth rate, reactive oxygen species (ROS) generation, and membrane damage were assessed using flow cytometry (FCM). Additionally, NPs bioavailability was investigated using single cell inductively coupled plasma mass spectrometry (SC-ICP-MS) as it allowed to distinguish between cellular Ce and Ti in mixture exposures. NPs characterization was performed using single-particle inductively coupled with plasma mass spectrometry (SP-ICP-MS). The use of SP-ICP-MS allowed the differentiation of NP size distributions within the mixtures, providing unique insights into their behavior and potential effects, when present in mixtures. Based on existing literature, our initial hypothesis was that the toxicity of TiO_2-NPs and CeO_2-NPs mixtures would likely be reduced due to specific physicochemical interactions between the NPs, such as hetero-aggregation, which are expected to limit the extent to which NPs contact or enter algal cells, thereby reducing the observed toxic effects in mixture exposures compared to individual NPs exposures.

2. Materials and methods

2.1. Nanoparticles and suspension preparation

The nano-powders of TiO_2 (NM-102-JRCNM10202) and CeO_2 (NM-212-JRCNM02102) were acquired from the Nanomaterials Repository at the European Commission Joint Research Centre, Ispra, Italy. Detailed information on the characteristics of these NPs, including their composition, primary size, water solubility, zeta potential, agglomeration/aggregation behavior, coating and surface chemistry, photocatalytic activity, and redox potential can be found in previous publications for TiO_2-NPs (Rasmussen et al., 2014) and for CeO_2-NPs (Singh et al., 2014). Both NPs are comparable in nominal sizes but exhibit markedly different physicochemical and redox properties that could influence their behavior and effects on algae.

The stock suspensions of 3000 mgL^{-1} were prepared by adding 15 mg of TiO_2/CeO_2-NPs to 5 mL of ultrapure water (Milli-Q Advantage, Molsheim, France) in glass vials. Then, the suspensions were sonicated for 15 min (40 KHz) (Branson 5510 MT Ultrasonic Cleaner, Branson Ultrasonics Corporation, Danbury, USA). In addition, ionic Ti at a concentration of 998 ± 2 mg L^{-1} (Fluka Analytical, Buchs, Switzerland) was used for analysis by ICP-MS. Gold nanoparticles (Au-NPs) with a size of 50.2 nm and a concentration of 0.5 mg L^{-1} (Nanocomposix, San Diego, CA, USA) were employed to determine the transport efficiency (TE) in SP-ICP-MS and SC-ICP-MS analyses.

2.2. Characterization of suspension of TiO_2-NPs and CeO_2-NPs and their mixtures

The suspensions of TiO_2-NPs, CeO_2-NPs and their mixture in ultrapure water and exposure medium were characterized in terms of size distribution, aggregation and dissolution to ensure a comprehensive understanding of their behavior at 72 h. The size distribution of the NPs and their mixtures was analyzed using SP-ICP-MS (Agilent 7700 ICP-MS, Morges, Switzerland). The acquisition parameters are shown in **Table S1,** Supplementary Information (SI). Prior to analysis, instrument performance was optimized with 1 µg L^{-1} of Ce, Co, Li, Mg, Tl, Y in 2 % HNO_3. The sample flow rate, determined by gravimetry, and the transport efficiency (TE) were obtained prior to analyzing the samples. TE was calculated using the frequency method (Pace et al., 2011) with a suspension of 50 nm AuNPs with a concentration of 4.36×10^7 particles mL^{-1}. For the analysis of TiO_2-NPs, a calibration curve between 0 and 5 µg L^{-1} of ionic Ti in 1 % of HNO_3 was used. For the analysis of CeO_2-NPs, a calibration curve between 0 and 5 µg L^{-1} with the same particles was utilized since the behavior of NPs and the ionic form is different (Sanchez-Garcia et al., 2016). In addition, the hydrodynamic size distribution and zeta potential values were obtained by dynamic light scattering (DLS, Zetasizer Nano, Malvern Panalytical, Netherlands).

2.3. Bioassays with green alga R. subcapitata

2.3.1. Algal culture

R. subcapitata was cultured in Tris-acetate-phosphate (TAP) medium, pH of 7.0, whose composition is in **Table S2** in SI, starting with an initial cell density of 5×10^4 cell mL^{-1}. The culture was carried out in a specialized incubator (Infors HT Multritron, Infors, Basel, Switzerland) maintained at 20.1 °C with shaking at 100 rpm and a 16:8 h light-dark cycle (light intensity 60 µmol photons m^{-2} s^{-1}). After 72 h, at the middle of the exponential growth phase, the algal culture was gently centrifuged at 1300 ×*g* for 10 min (Multifuge X Pro Series centrifuge, Thermo Fisher, New Jersey, USA). The resulting pellet of the cells was collected

and resuspended in TAP exposure medium, whose composition is in **Table S3**, supplemented with varying concentrations of TiO_2-NPs, CeO_2-NPs and their mixtures. The initial cell concentration of the exposure experiment was adjusted to 3×10^5 cells mL^{-1} (Bakir et al., 2024). The exposure was carried out in the same conditions as the culture of the algae described before.

2.3.2. Assessment of the mixture toxicity

To study the effect of the mixture of TiO_2-NPs and CeO_2-NPs, a methodology based on the conversion to TUs was employed. TUs concept provides a standardized and quantitative framework for assessing mixture toxicity (Wang et al., 2020; Ye et al., 2018). The EC_{50} determined from the individual exposure to TiO_2-NPs and CeO_2-NPs were used for calculating the TU, following Eq. 1:

$$TU = \frac{C_i}{EC_{50_i}} \quad (1)$$

where C_i is the concentration of the NPs i and EC_{50_i} is the corresponding EC_{50} of the NPs i. Therefore, when TU is 1, this corresponds to the EC_{50}. Besides, the TU of the mixture is $TU_{mixture} = TU_i + TU_j$ with i and j corresponding to different materials used in the mixture. Various ratios of NP concentrations, all designed to achieve a $TU_{mixture}$ of 1 were employed. The ratios were calculated based on the EC_{50} values obtained from individual treatments with TiO_2-NPs or CeO_2-NPs as presented in **Fig. S1** and in our previous study (Bakir et al., 2025). EC_{50} concentration obtained for TiO_2-NPs was 28.3 ± 1.16 mg L^{-1}, while for CeO_2-NPs was 13.6 ± 0.57 mg L^{-1}. The following mixtures of TiO_2 and CeO_2-NPs have been tested: 14.2 mg L^{-1} TiO_2-NPs + 6.73 mg L^{-1} CeO_2-NPs (C1 mixture), 28.3 mg L^{-1} TiO_2-NPs + 13.6 mg L^{-1} CeO_2-NPs (C2 mixture), 18.8 mg L^{-1} TiO_2-NPs + 4.6 mg L^{-1} CeO_2-NPs (C3 mixture), 9.41 mg L^{-1} TiO_2-NPs + 9.27 mg L^{-1} CeO_2-NPs (C4 mixture). Although the concentrations tested in this study are considerably higher than those typically found in natural environments (e.g. <100 ng L^{-1} for Ce-NPs; and < 10 µg L^{-1} for Ti-NPs) (Azimzada et al., 2021), they were chosen based on regulatory and ecotoxicological relevance.

2.3.3. Ecotoxicity testing

The choice of alga *Raphidocelis subcapitata* was based on the recommendation of the Organization for Economic Co-operation and Development (OECD) for conducting ecotoxicity tests (OECD, 2011). The tests were carried out in glass flasks. The effects of TiO_2-NPs, CeO_2-NPs and their mixtures on *R. subcapitata* were evaluated based on their impact on algal growth, intracellular ROS generation and membrane integrity. Growth rate inhibition was determined by measuring cell numbers using FCM (BD Accuri C6 Plus flow cytometer, BD, New Jersey, USA) after 72 h of exposure. A threshold of 20,000 events within the algae gate in the chlorophyll autofluorescence cytogram was applied. The gating strategy allowing the distinction between the algae and NPs aggregates of comparable size is detailed in SI (**Fig. S2**). Exposure to 10 µg L^{-1} Ag^+ as a $AgNO_3$ was used as a positive control and resulted in 100 % growth inhibition.

The effect of the treatments on the membrane integrity of the algal cell was determined using FCM following staining with propidium iodide (PI) following an optimized procedure (Beauvais-Fluck et al., 2017; Santos et al., 2024). After 72 h of exposure to the NPs and their mixtures, PI was added to the algae to a final concentration of 7 µM. The samples were incubated in the dark for 30 min before analysis using FCM on channel FL-2. Cells heated at 90 °C for 30 min in the dark served as positive control. Unexposed cells treated identically to the samples were used as negative controls.

The effect of the NPs and their mixtures on the intracellular ROS level was assessed using Synergy H1 microplate reader (Biotek, Santa Clara, USA). Algal cells were stained with 10 µM CellROX® Green reagent (Thermo Fisher Scientific, Waltham, MA, USA) and incubated in the dark at 37 °C for 1 h. Cells exposed to 20 % hydrogen peroxide for 30 min were used as positive controls and resulted in more than 80 % of affected cells. Following exposure and reagent addition, fluorescence was measured with an excitation wavelength of 488 nm and an emission wavelength of 530 nm.

2.3.4. Bioavailability of the NPs and their mixtures to algae

The bioavailability of the NPs and their mixtures was assessed in terms of the adsorbed (ethylenediaminetetraacetic acid (EDTA)-extractable) and intracellular (EDTA non-extractable) amount of Ti and Ce in each cell determined by SC-ICP-MS (Perkin Elmer NexION 2000 (Perkin Elmer, Toronto, Canada) with an Asperon™ linear pass spray chamber (Perkin Elmer, Toronto, Canada) and a flow-focusing nebulizer (Ingeniatrics, Sevilla, Spain)). For the sample introduction, a µDx Single Cell Autosampler (Elemental Scientific, Omaha, NE, USA) was used, which operated with a syringe pump at a rate of 10 µL min^{-1}. To determine transport efficiency, the frequency method was used. Since it is not possible to obtain reference material of size comparable with those of algae, 50 nm AuNPs have been used to determine the mass of the element per cell (Suarez-Oubina et al., 2023).

Following 72 h of exposure, the algae were centrifugated (1300 ×g for 10 min) and the cell pellets were collected. The pellets were rinsed with 0.02 M EDTA to discriminate between adsorbed and intracellular metal (Kosak Nee Rohder et al., 2018). To do that, the cell pellets were resuspended in 0.02 M EDTA, and the suspensions were centrifuged. The resultant supernatant was discarded, and the pellet was washed with TAP exposure medium. This procedure was repeated 5 times. The rinsed cell pellets were lyophilized and resuspended in 50 mL of ultrapure water. Before the analysis, the instrument was optimized with a solution of 1 µg L^{-1} of Be, Ce, Fe, In, Li, Mg, Pb and U, provided by the manufacturer. Subsequently, the acquisition parameters for both elements were optimized to get the maximum sensitivity with a solution of 5 µg L^{-1} of Ti in 1 % of HNO_3 and 1 µg L^{-1} of CeO_2-NPs. For the analysis of algae exposed to TiO_2-NPs, due to the likely Ca and P interferences, ammonia was used as a reaction gas in the reaction cell. The parameters of the reaction cell were optimized before the analysis. To avoid the interferences, the m/z ratio 131, corresponding to $^{48}Ti(NH)(NH_3)_4$) was measured since no interferences were observed with this adduct (Suárez-Oubiña et al., 2022). The interferences with Ca were also studied with suspensions of 5 µg L^{-1} of Ti and an increasing concentration of Ca from 10 µg L^{-1} to 10 mg L^{-1}, confirming non-relevant interferent effects from 1 mg L^{-1} of Ca. Since no interferences were expected for CeO_2, measurements were performed in standard mode. Since the behavior of the ionic Ce is different from that of CeO_2-NPs (different slopes for the calibration curves: 5.55×10^4 for ionic Ce and 3.02×10^4 for CeO_2-NPs), a calibration curve of CeO_2-NPs was used for the quantification. The acquisition parameters are in **Table S4**. Additionally, untreated cells and cells treated with TiO_2-NPs, CeO_2-NPs and their mixtures were visualized using a digital microscope (VHX-X1, Keyence, Mechelen, Belgium).

2.4. Data analysis

All the experiments were carried out in triplicate. A one-way analysis of variance (ANOVA) was performed to test significant differences between the treatments. Prior to performing ANOVA, the assumptions of normality were tested using the Shapiro–Wilk test. Tukey's Honestly Significant Difference (HSD) test was applied as a post hoc comparison to determine pairwise differences between means. All analyses were performed using OriginPro 2023 (v. 9.6.5.169; OriginLab Corporation, Northampton, MA, USA), and differences were considered statistically significant at $p < 0.05$.

3. Results and discussion

3.1. Characterization of the suspension of TiO_2-NPs, CeO_2-NPs and their mixtures

For TiO_2-NPs suspension in exposure medium, SP-ICP-MS indicated a particle size of 52 ± 8 nm (LOD_{size} of 30 nm) but bigger aggregates with sizes until 400 nm were also detected (Fig. 1a), like the ultrapure water suspension (**Fig. S3**). The zeta potential obtained for TiO_2-NPs was −9.50 ± 2.37 mV. For CeO_2-NPs suspension in exposure medium, SP-ICP-MS (Fig. 1b) indicated a mean particle size of 77 ± 9 nm, with aggregates around 100–200 nm. These values align with previous literature, which reported primary particle sizes of 28 nm detected by transmission electron microscopy (TEM), with aggregates around 100 nm (Singh et al., 2014). The obtained LOD_{size} was 24 nm, confirming the presence of smaller particles. No dissolution was observed at any of the concentrations studied (from 10 to 30 mg L^{-1}) as the measured dissolved concentrations were below the dissolution limit of detection (LOD_{diss}) of 5.14 ng L^{-1}. Similarly, no dissolution was found in the CeO_2-NP suspensions LOD_{diss} of 0.44 ng L^{-1}. The zeta potential was - 6.55 ± 2.30 mV. No dissolution was detected in either of the mixtures.

For mixtures suspended in TAP medium, SP-ICP-MS detected mean most frequent particle sizes: 92 ± 8 nm for TiO_2-NPs and 78 ± 6 nm for CeO_2-NPs (Fig. 1). For TiO_2-NPs, the size distribution shifted toward larger sizes in the mixtures in comparison with individual treatments, indicating that aggregation was more likely when the TiO_2-NPs were combined with CeO_2-NPs. For CeO_2-NPs, the distribution for the mixture remained like the one obtained for the individual suspension. DLS measured larger apparent hydrodynamic sizes than SP-ICP-MS (**Fig. S3**) because DLS reflects intensity-weighted hydrodynamic diameters influenced by particle–medium interactions, whereas SP-ICP-MS provides element-specific, number-weighted particle sizes. Because DLS cannot distinguish between Ti- and Ce-containing particles, it cannot resolve the aggregation behavior of each component in the mixed suspension. Therefore, quantitative assessment of aggregation in the exposure medium and in mixtures relied on the element-specific resolution of SP-ICP-MS.

Studies have shown that when metal oxide NPs are mixed, they tend to interact through van der Waals forces, electrostatic interactions, and bridging via ions in the medium (Keller et al., 2010). In particular, TiO_2-NPs and CeO_2-NPs have been reported to form hetero-aggregates, leading to increased hydrodynamic sizes in mixtures compared to individual suspensions, which was dependent on CeO_2-NPs/TiO_2-NPs ratio (Luo et al., 2017). Additionally, CeO_2-NPs, which can have higher affinity for binding due to surface oxygen vacancies and variable charge states (Ce^{3+}/Ce^{4+}) (Mohajeri et al., 2025), may act as "nucleation centers," promoting aggregation with TiO_2-NPs. Such aggregation shifts the size distributions toward larger size for TiO_2-NPs in mixtures, could result in limiting direct contact with algal cells and decreasing their bioavailability and effects.

3.2. Effects of TiO_2-NPs, CeO_2-NPs, and their mixtures on algae

The effects of TiO_2-NPs, CeO_2-NPs, and their mixtures on algae were evaluated in terms of growth inhibition, ROS generation, and membrane damage. Except for the exposure to C2 mixture, where the TU_{exp} is 2 (indicating 100 % of growth inhibition), the expected growth inhibition for all other exposures is 50 % since $TU_{mixture}$ value of 1. Opposite to this expectation, antagonistic interactions were observed, as the growth inhibition was lower than expected based on TUs. Specifically, when the algae were exposed to mixture of NPs, the induced growth inhibition decreased compared to the effects observed with the individual NPs (Fig. 2a). Although the EC_{50} of TiO_2-NPs alone was 28 mg L^{-1}, a hormesis effect was observed (**Fig. S1**) when algae were exposed to concentrations ranging from 10 to 20 mg L^{-1}. The factors driving hormesis response remain largely unexplored (Keller and Slaveykova, 2025); however, mild stress induced by TiO_2-NPs can trigger adaptive cellular mechanisms, including the accumulation of ROS, production of antioxidant metabolites, and increased activity of antioxidant enzymes (Agathokleous et al., 2019; Agathokleous et al., 2022). When exposed to 28 mg L^{-1} of TiO_2-NPs combined with 14 mg L^{-1} CeO_2-NPs (C2 mixture) the growth inhibition was 12.3 ± 4.5 %, despite the expectation of complete growth inhibition ($TU_{mixture}$ of 2).

To assess the strength of antagonistic interaction, or deviation from additivity, ΔTU (TU_exp–TU_obs) was calculated among different treatments (**Table S5**). When comparing expected inhibition with ΔTU, C2 mixture, which had the highest expected inhibition (100 %), also exhibited the largest ΔTU (1.76). The other mixtures (C1, C3, C4), all with expected inhibition of 50 %, showed intermediate ΔTU values ranging from 0.66 to 1.0, indicating a moderate positive relationship between expected inhibition and ΔTU. These antagonistic effects can be attributed to the interactions between the NPs, which may result in the formation of hetero-aggregates, potentially reducing the bioavailability of the NPs to algae (Schiavo et al., 2018). This explanation aligns with the shift in size distribution toward larger sizes observed in the mixtures for TiO_2-NPs (Fig. 1).

It is worth noting that the control growth rate in TAP medium (0.85 ± 0.07 day^{-1}) was lower than the OECD 201 guideline minimum (≥1.4 day^{-1}) due to reduced nutrients and light to maintain NPs stability. Slower algal growth can alter the NPs-to-cell ratio and increase adsorption or hetero-aggregation at the cell surface, as seen for CeO_2-NPs (Schiavo et al., 2018). While the absolute magnitude of effects may

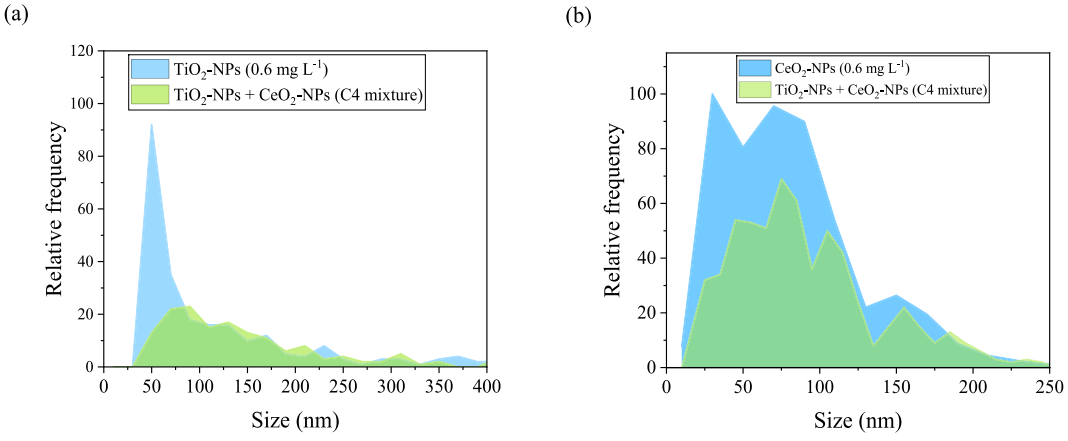

Fig. 1. Size distribution of NPs in mixture and individual suspensions obtained by SP-ICP-MS in exposure medium (a) Ti signal - 0.6 mg L^{-1} of TiO_2-NPs and C4 mixture; (b) Ce signal - 0.6 mg L^{-1} of CeO_2-NPs and C4 mixture.

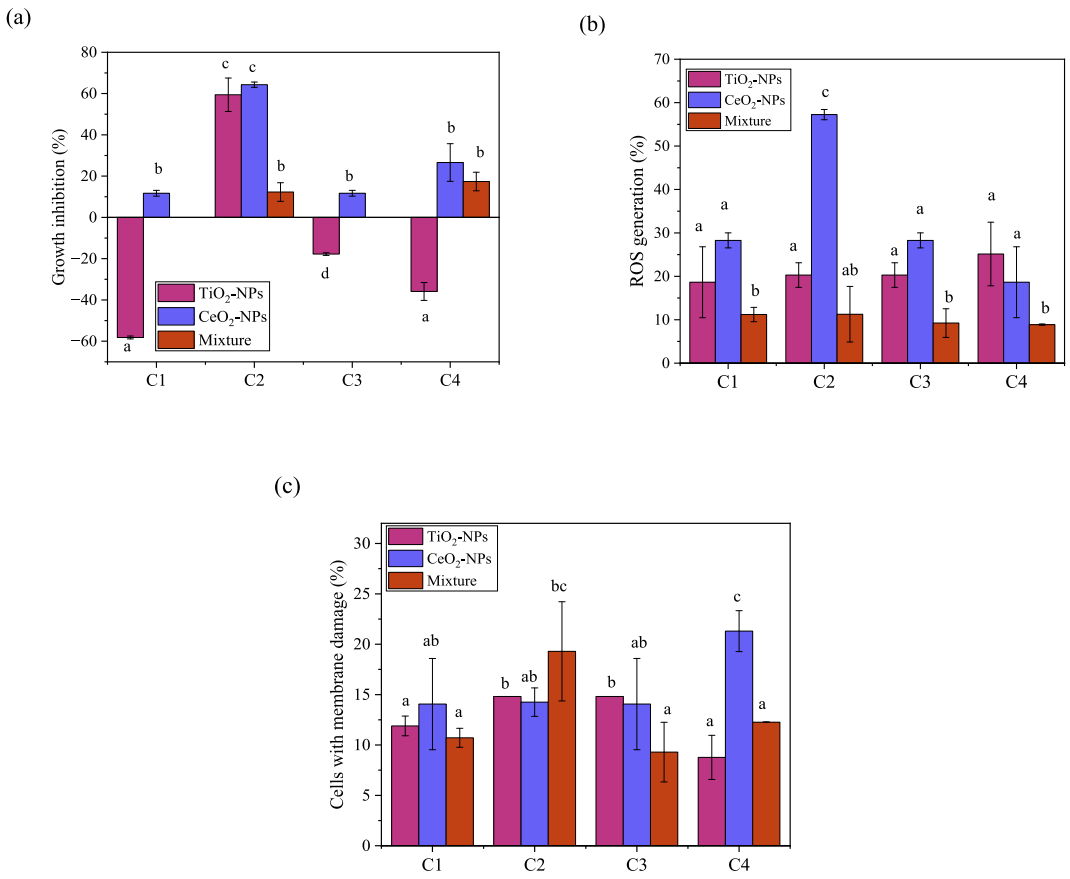

Fig. 2. Effect of different mixtures and single exposures of TiO_2-NPs and CeO_2-NPs on **(a)** growth inhibition, **(b)** ROS generation, and **(c)** membrane damage in the green alga *R. subcapitata* ($\bar{x}\pm SD$). Exposure duration of 72 h. Tested mixtures: 14.2 mg L^{-1} TiO_2-NPs + 6.73 mg L^{-1} CeO_2-NPs (C1 mixture), 28.3 mg L^{-1} TiO_2-NPs + 13.4 mg L^{-1} CeO_2-NPs (C2 mixture), 18.8 mg L^{-1} TiO_2-NPs + 4.6 mg L^{-1} CeO_2-NPs (C3 mixture), 9.41 mg L^{-1} TiO_2-NPs + 9.27 mg L^{-1} CeO_2-NPs (C4 mixture). The letters indicate the significant differences between the exposures, as obtained by one-way ANOVA followed by a Tukey test ($p < 0.05$, $n = 3$). (For interpretation of the references to colour in this figure legend, the reader is referred to the web version of this article.)

differ from standard OECD conditions, all treatments were performed under identical conditions, so the observed antagonistic interactions between TiO_2-NPs and CeO_2-NPs reflect particle interactions under particle-stable conditions.

The above observations align with the literature reporting antagonistic effects in mixtures of TiO_2-NPs, ZnO-NPs and CeO_2-NPs on bacterium *Nitrosomas europea*, where TiO_2-NPs reduced the bioavailability and consequently mitigated the toxicity of CeO_2-NPs (Yu et al., 2016b) or ZnO-NPs (Yu et al., 2016a). A similar reduction in bioavailability was also identified as the cause of the antagonistic interactions of TiO_2-NPs and CeO_2-NPs on human hepatic cells (Rosario et al., 2022). Zebrafish embryos exposed to a combination of TiO_2-NPs and CeO_2-NPs also exhibited antagonistic interactions, with no noticeable developmental effects, contrasting with the results from single exposures (Pecoraro et al., 2023). A reduction in the influence of ZnO-NPs by TiO_2-NPs was also seen in zebrafish embryos (Hua et al., 2016). For green algae, antagonistic effects have been observed in *Chlorella* sp. exposed to different crystalline forms of TiO_2-NPs (anatase and rutile) (Iswarya et al., 2015), suggesting that similar bioavailability-based mechanisms may operate across diverse organisms. However, differences in the observed effects among the organisms likely reflect species-specific sensitivity and exposure pathways. For example, algae are primarily affected via direct particle-cell interactions in the aqueous phase, whereas fish embryos may experience additional uptake and internalization pathways, influencing the manifestation of antagonism. The present results contrast with the synergistic effect observed in other studies. For example, a mixture of TiO_2-NPs, SiO_2-NPs and ZrO_2-NPs caused oxidative stress and mitochondrial damage in the alga *S. obliquus* (Liu et al., 2018), while fluorescent nanoplastics enhanced the toxicity of TiO_2-NPs in *S. obliquus* by reducing photosynthetic yield (Das et al., 2022). Synergistic effects were also reported for binary mixtures of TiO_2-NPs with CdS, ZnS or SiO_2-NPs in another alga *H. akashiwo* attributed to the "Trojan horse" mechanism of TiO_2-NPs increasing the bioavailability of the other metal NPs (Pikula et al., 2022). In contrast, additive effects were observed for a mixture of TiO_2 -NPs and nanotubes in *S. obliquus* (Wang et al., 2020).

The formation of ROS and oxidative stress are major toxicity mechanisms (von Moos and Slaveykova, 2014) which have been reported for individual treatments with CeO_2-NPs (Angel et al., 2015; Liu et al., 2024) or TiO_2-NPs and different microorganisms (Fu et al., 2015; Li et al., 2015; Liu et al., 2022; Neale et al., 2015; Xia et al., 2015). In the present study, an excessive ROS generation was observed in both mixture and individual treatments (Fig. 2**b**). The values in mixtures were statistically significantly lower than in the individual treatments, exhibiting antagonistic interactions as was observed in algal growth inhibition tests. Given that CeO_2-NPs are known for their redox cycling between Ce^{3+} and Ce^{4+} states, which confers intrinsic antioxidant properties (Dhall and Self, 2018; Mohajeri et al., 2025), it can be hypothesized that, in mixed exposures, CeO_2-NPs may scavenge ROS, thereby mitigating the oxidative stress induced by TiO_2-NPs and reducing cellular oxidative damage and membrane disruption. TiO_2-NPs, commonly in mixed anatase/rutile crystalline form, possess a band gap in the range of ~3.0–3.2 eV and display strong photocatalytic activity, producing ROS (Gatou et al., 2024) and thus acting as oxidative stress inducers. The above observations are consistent with previous studies reporting a decrease in the ROS levels induced by a mixture of

TiO_2-NPs and TiO_2 nanotubes compared with the single exposure for *S. obliquus* (Wang et al., 2020). TiO_2-NPs decreased the oxidative stress and the membrane damage caused by Hg in *C. reinhardtii* (Li et al., 2020). However, for *C. pyrenoidosa*, the value obtained was higher for the mixture than for the single exposure (Wang et al., 2020). This increase in ROS could lead to peroxidation of the lipid membrane, which could cause damage to the membrane (Liu et al., 2024), allowing the internalization of the NPs. Indeed, individual exposure to TiO_2-NPs, CeO_2-NPs and their mixtures resulted in a significant increase of the algal cells with damaged membranes in comparison with untreated controls (Fig. 2c). For the single TiO_2-NPs exposure, the percentage of cells with membrane damage was between 13 and 17 %, meanwhile, for CeO_2-NPs, the values were between 14 and 21 %. When the algae were exposed to the mixture of the NPs, the percentage obtained was between 9 and 19 %. The higher percentage corresponded to the mixtures where there was significant growth inhibition (C2 and C4 mixtures). For C4 mixture, the percentage of membrane-damaged cells (12.3 ± 0.1 %) was lower than that for a single exposure of CeO_2-NPs (21.3 ± 2.0 %), confirming the observed antagonistic interactions on growth inhibition and ROS generation. For the remaining mixtures, no significant differences were observed between the mixtures and their corresponding concentrations in the single exposures.

3.3. Bioavailability of TiO_2-NPs, CeO_2-NPs and their mixtures

The bioavailability of TiO_2-NPs and CeO_2-NPs was determined for all mixture and individual treatments by measuring the intracellular (EDTA non-extractable) titanium and cerium concentrations by SC-ICP-MS (Fig. 3a). For TiO_2-NPs, single exposures yielded 15.7–24.3 fg Ti $cell^{-1}$, while mixtures decreased to 12.9–15.9 fg Ti $cell^{-1}$. CeO_2-NPs showed 3.6–8.6 fg Ce $cell^{-1}$ in single exposures, dropping to 2.7–4.4 fg Ce $cell^{-1}$ in mixtures. Specifically, the highest single-exposure intracellular masses observed under single NP exposure (24.3 fg Ti $cell^{-1}$ and 8.6 fg Ce $cell^{-1}$), decreased to 13.1 fg Ti $cell^{-1}$ and 4.4 fg Ce $cell^{-1}$, respectively, when NPs were present in C2 mixture.For exposure to C2 and C4 mixtures, the intracellular mass of Ce was lower than the one obtained for exposure to individual NPs. In the case of Ti, a differences in the mean intracellular mass was observed only in the C4 mixture exposure compared with the other mixtures. This increase in the Ti intracellular concentrations could explain the inhibition of the growth found for C4 mixture exposure (Fig. 2a). However, for algae exposed to C2 mixture, another mechanism should be the reason since the values of the intracellular contents were the same as the ones obtained for the other two mixtures. These findings indicate that the presence of one NP type can influence the internalization of the other, highlighting the importance of considering NPs interactions in mixed exposure studies.

The adsorption of NPs on the cell may also affect the growth inhibition. To explore this hypothesis, the cells before the EDTA washing cycle were also analyzed (Fig. 3b). C2 and C4 mixtures had higher values of cerium adsorbed, which corresponds to the mixtures which produced toxicity on the cells, although no correlation between the mass of Ce and the growth inhibition values was obtained (**Fig. S4**). Although C2 mixture presented higher values of NPs attached to the cells, for C4 mixture, only 13 % of the total Ti was absorbed on the cells. This suggests that the toxicity of these mixtures is not directly correlated with the mass of the internalized or adsorbed element (**Fig. S4**).

Adsorption of NPs to the algal surface was also evident in the brightfield images (Fig. 4), where large aggregates were observed. In the mixture of C1, a slightly lower amount of cellular Ti was detected compared to the single exposure. Conversely, for the C2 mixture, the bioavailability of both Ti and Ce was lower than in the single exposure, which may explain the competitive and antagonistic interactions observed for growth inhibition, ROS generation and membrane damage. Since the cells were rinsed prior to analysis, it can be inferred that the measured Ti and Ce were internalized within the cells. However, these values should be interpreted with caution, as the distinction between intracellular and surface-adsorbed NP fractions is operationally defined by the EDTA rinse step. The internalization was identified previously as a mechanism of toxicity for *R. subcapitata* exposed to 20–40 nm TiO_2-NPs (Ozkaleli and Erdem, 2018). However, for CeO_2-NPs, our results differ from the literature, where no internalization in algal cells was observed. Instead, rapid adsorption to the membrane, causing morphological changes in the cells, was reported (Kosak Nee Rohder et al., 2018; Mackevica et al., 2023; Manier et al., 2013). In contrast, for other green alga *C. reinhardtii*, internalization of uncoated 4 nm-sized CeO_2-NPs was observed due to damage in the cell wall/ membrane, enabling NPs internalization (Pulido-Reyes et al., 2019).

The inhibition of the growth due to the entrapment of the cells in aggregates of both NPs was also described (Ghazaei and Shariati, 2020; Hund-Rinke et al., 2020; Liu et al., 2024; Manier et al., 2013; Xia et al., 2015). For example, for TiO_2-NPs single exposure, the entrapment of algae in NPs aggregates was the cause of the damage to the cell membranes (Ghazaei and Shariati, 2020; Wang et al., 2024a). For CeO_2-NPs, cell damage was also obtained because of the adsorption of NPs to *R. subcapiatata* (Angel et al., 2015). For *Chlorella vulgaris* exposed to 10–20 nm CeO_2-NPs, the membrane damage was caused by oxidative stress and physical damage (Liu et al., 2024). In the present study, particles attached to the cells were observed in both single and mixture

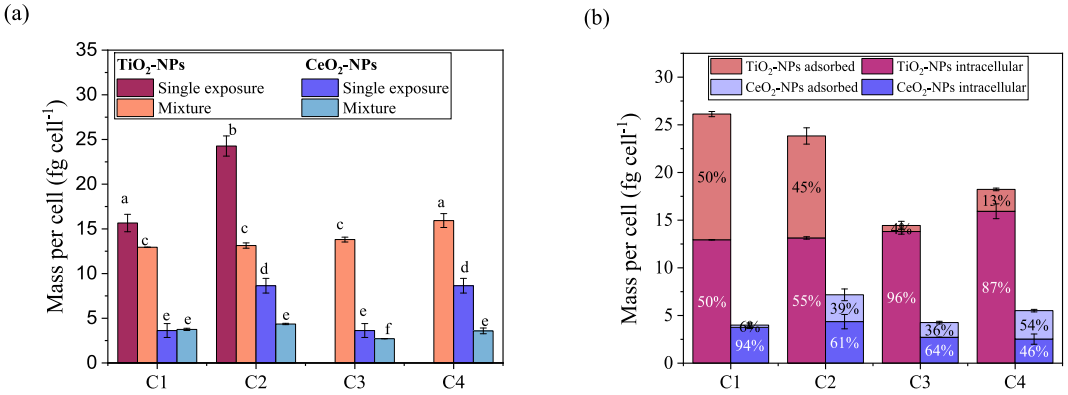

Fig. 3. Bioavailability of titanium and cerium by SC-ICP-MS (fg $cell^{-1}$) to the green alga *R. subcapitata* ($\bar{x}$±SD). (**a**) Mass of titanium and cerium per cell corresponded to the intracellular (EDTA non-extractable) fraction for the mixture and the single exposure (equivalent concentration used for the mixtures). (**b**) Comparison of the mean mass of titanium and cerium per cell of the adsorbed (EDTA extractable) and intracellular fractions. Tested mixtures: 14.2 mg L^{-1} TiO_2-NPs + 6.73 mg L^{-1} CeO_2-NPs (C1 mixture), 28.3 mg L^{-1} TiO_2-NPs + 13.4 mg L^{-1} CeO_2-NPs (C2 mixture), 18.8 mg L^{-1} TiO_2-NPs + 4.6 mg L^{-1} CeO_2-NPs (C3 mixture), 9.41 mg L^{-1} TiO_2-NPs + 9.27 mg L^{-1} CeO_2-NPs (C4 mixture). The letters indicate the significant differences between the exposures, as obtained by one-way ANOVA followed by a Tukey test ($p < 0.05$, $n = 3$). (For interpretation of the references to colour in this figure legend, the reader is referred to the web version of this article.)

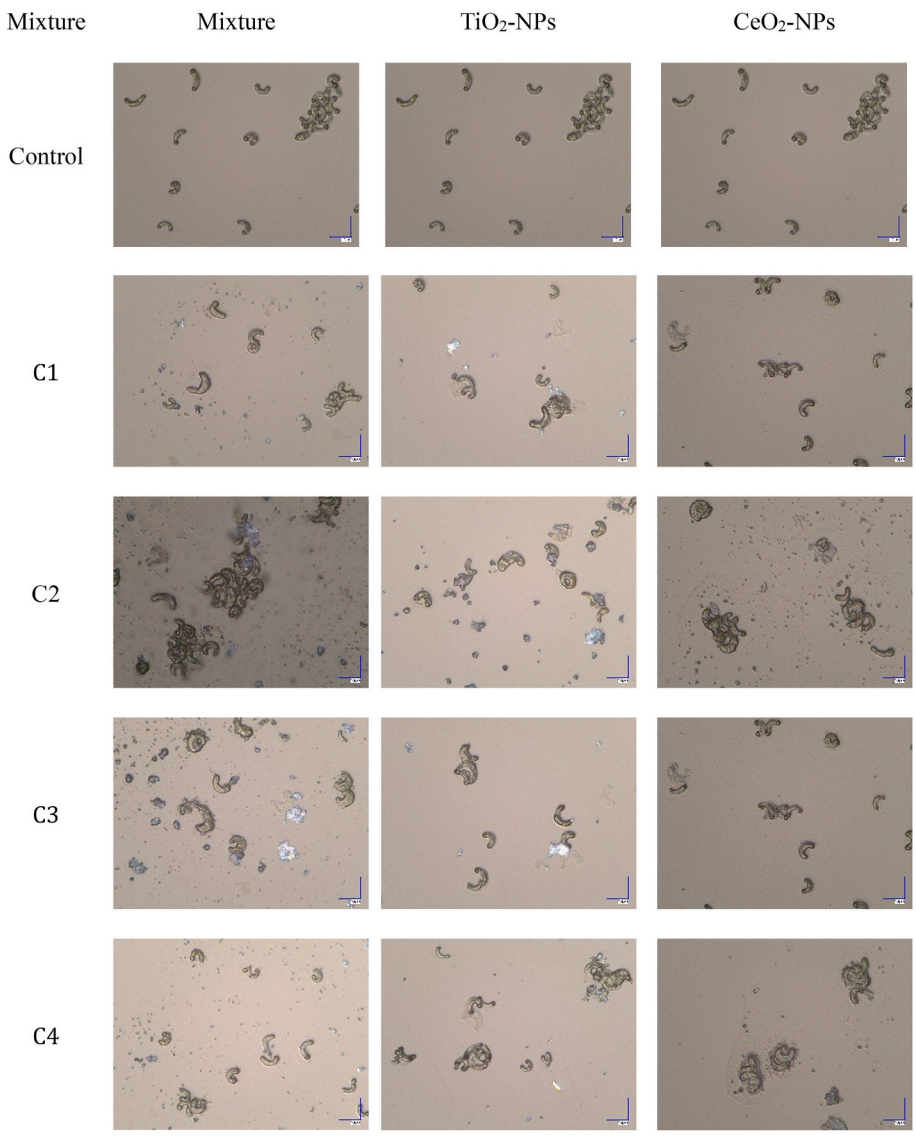

Fig. 4. Digital microscope images obtained for the green alga *R. subcapitata* exposed to TiO_2-NPs, CeO_2-NPs and their mixtures for 72 h. Tested mixtures: 14.2 mg L^{-1} TiO_2-NPs + 6.73 mg L^{-1} CeO_2-NPs (C1 mixture), 28.3 mg L^{-1} TiO_2-NPs + 13.4 mg L^{-1} CeO_2-NPs (C2 mixture), 18.8 mg L^{-1} TiO_2-NPs + 4.6 mg L^{-1} CeO_2-NPs (C3 mixture), 9.41 mg L^{-1} TiO_2-NPs + 9.27 mg L^{-1} CeO_2-NPs (C4 mixture). (For interpretation of the references to colour in this figure legend, the reader is referred to the web version of this article.)

exposures (Fig. 4). In all the individual and mixture treatments, hetero-aggregates of algae with NPs were observed, with larger aggregates for C2 mixture (20–40 μm) compared to the other mixtures (around 14 μm). The trapping of the algae cells within the NPs aggregates has been shown to contribute to the toxicity of TiO_2-NPs to *R. subcapitata* (Joonas et al., 2019), due to the reduced nutrient bioavailability and shading effect (Ghazaei and Shariati, 2020; Hund-Rinke et al., 2020; Xia et al., 2015). Additionally, the attachment of NPs to algae cells can cause damage to the cell wall, facilitating the internalization of NPs by *R. subcapitata* (Angel et al., 2015; Hund-Rinke et al., 2020; Mahaye and Musee, 2023; Ozkaleli and Erdem, 2018). Titanium particles were found attached to the cell walls and inside the chloroplasts of the alga dinoflagellate *Karenia brevis* (Li et al., 2015). In *C. reinhardtii* cells were trapped in aggregates of TiO_2-NPs with a primary size of nanometers, but this phenomenon was not observed for TiO_2-NPs with sizes of 15 and 20 nm (Liu et al., 2022). Similarly, direct contact of CeO_2-NPs with cyanobacterium *Microcystis aeruginosa* led to cell wall damage and NP internalization (Wu et al., 2022).

Overall, the antagonistic interactions observed, where algal growth inhibition, ROS generation, and membrane damage were lower in mixtures of TiO_2-NPs and CeO_2-NPs than in single NP exposures, highlight that complex physicochemical processes modulate NPs toxicity. This study provides an insight into mixture effects, offering a novel understanding of NPs interactions, bioavailability, and toxicity modifications, particularly in environments where multiple NPs coexist. Employing a TU-based approach enabled the identification of additive, antagonistic and synergistic interactions and could support predictive extrapolation to contaminated hotspots, informing both risk assessment and regulatory strategies. Although the tested concentrations exceed typical environmental levels, the results highlight patterns of combined toxicity at the organismal level. Future work should integrate molecular and cellular endpoints, environmentally realistic conditions, and longer-term or multigenerational studies to enhance ecological relevance, improve predictive modelling, and guide the design of safer nanomaterials and management of NPs-contaminated ecosystems.

4. Conclusions

This study demonstrates that interactions between TiO_2-NPs and CeO_2-NPs can modulate toxicity, with mixture exposures producing lower growth inhibition, ROS generation, and membrane damage than single-NP treatments. By combining a TU-based approach with single-cell and single-particle techniques, such as flow cytometry, SP-ICP-MS, and SC-ICP-MS, we provide advanced insight into NPs mixture toxicity in aquatic environments. Antagonistic effects in growth inhibition observed in algae exposed to the mixtures of TiO_2-NPs and CeO_2-NPs likely reflect hetero-aggregation and reduced bioavailability, as SC-ICP-MS confirmed lower intracellular or adsorbed mass per cell compared to individual exposures. Adsorption to the cell surface, increased ROS generation and cell wall damage were observed for both single and mixture treatments. SP-ICP-MS revealed that TiO_2-NPs size distributions shifted toward larger aggregates in mixtures, while CeO_2-NPs remained like single exposures. No dissolution was detected under the conditions tested. These findings highlight the complexity of NPs interactions, the importance of considering mixture effects in ecological assessments, and the relevance for contaminated hotspots. Future studies incorporating molecular endpoints, environmentally realistic conditions, and longer-term exposures will further enhance ecological relevance, improve risk assessment, and inform safer nanomaterial design.

CRediT authorship contribution statement

Mariam Bakir: Writing – original draft, Visualization, Methodology, Investigation, Formal analysis, Conceptualization. **Isabel Abad-Alvaro:** Writing – review & editing, Validation, Methodology. **Francisco Laborda:** Writing – review & editing, Validation, Supervision, Resources. **Vera I. Slaveykova:** Writing – review & editing, Validation, Supervision, Resources, Project administration, Investigation, Funding acquisition, Conceptualization.

Declaration of competing interest

The authors declare that they have no known competing financial interests or personal relationships that could have appeared to influence the work reported in this paper.

Acknowledgements

The authors acknowledge the financial support of Swiss National Science Foundation Lead Agency with US, Project 320030L-227440, the European Commission Joint Research Centre Nanomaterials Repository for providing the nanomaterials, as well as Dr. Jorge Cors from the Department of Quantum Matter Physics at the University of Geneva for granting access to the digital microscope and the Servicio General de Apoyo a la Investigación-SAI, Universidad de Zaragoza. IA thanks the European Union-Next Generation EU and the Spanish Ministry of Universities for funding under the María Zambrano Grant (MZ-240621). FL acknowledge the financial support of Spanish Ministry of Science and Innovation (project PID2021-123203OB-I00), and the Government of Arago (project E29_23R).

Appendix A. Supplementary data

Supplementary data to this article can be found online at https://doi.org/10.1016/j.impact.2025.100608.

Data availability

Data for this article, including NP characterization by SP-ICP-MS, effect of the MPs and their mixtures on algae obtained by FCM and bioavailability determined by SC-ICP-MS are available at YARETA at https://doi.org/10.26037/yareta:htnsrcqtmffjzo36ck2aoavdoa

References

Agathokleous, E., Feng, Z.Z., Iavicoli, I., Calabrese, E.J., 2019. The two faces of nanomaterials: a quantification of hormesis in algae and plants. Environ. Int. 131. https://doi.org/10.1016/j.envint.2019.105044.

Agathokleous, E., Wang, Q., Iavicoli, I., Calabrese, E.J., 2022. The relevance of hormesis at higher levels of biological organization: Hormesis in microorganisms. Curr. Opin. Toxicol. 29, 1–9. https://doi.org/10.1016/j.cotox.2021.11.001.

Angel, B.M., Vallotton, P., Apte, S.C., 2015. On the mechanism of nanoparticulate CeO_2 toxicity to freshwater algae. Aquat. Toxicol. 168, 90–97. https://doi.org/10.1016/j.aquatox.2015.09.015.

Azimzada, A., Jreije, I., Hadioui, M., Shaw, P., Farner, J.M., Wilkinson, K.J., 2021. Quantification and characterization of Ti-, Ce-, and ag-nanoparticles in global surface waters and precipitation. Environ. Sci. Technol. 55 (14), 9836–9844. https://doi.org/10.1021/acs.est.1c00488.

Bakir, M., Jimenez, M.S., Laborda, F., Slaveykova, V.I., 2024. Exploring the impact of silver-based nanomaterial feed additives on green algae through single-cell techniques. Sci. Total Environ. 939, 173564. https://doi.org/10.1016/j.scitotenv.2024.173564.

Bakir, M., Abad-Alvaro, I., Laborda, F., Slaveykova, V.I., 2025. Comparative assessment of uptake and effects of TiO_2 and CeO_2 nanoparticles in algae using advanced single-entity analytical techniques. Aquat. Toxicol. 286, 107430. https://doi.org/10.1016/j.aquatox.2025.107430.

Beauvais-Fluck, R., Slaveykova, V.I., Cosio, C., 2017. Cellular toxicity pathways of inorganic and methyl mercury in the green microalga *Chlamydomonas reinhardtii*. Sci. Rep. 7 (1), 8034. https://doi.org/10.1038/s41598-017-08515-8.

Book, F., Persson, M., Carmona, E., Backhaus, T., Lammel, T., 2022. Colloidal silica nanomaterials reduce the toxicity of pesticides to algae, depending on charge and surface area. Environ. Sci. Nano 9 (7), 2402–2416. https://doi.org/10.1039/d1en01180d.

Dar, G.I., Saeed, M., Wu, A., 2020. Toxicity of TiO_2-NPs. In: Wu, A., Ren, W. (Eds.), TiO_2 Nanoparticles: Applications in Nanobiotechnology and Nanomedicine. Wiley-VCH Verlag GmbH & Co. https://doi.org/10.1002/9783527825431. KGaA.

Das, S., Mukherjee, A., 2024. Combined effects of titanium dioxide nanoparticles and bisphenol-a on freshwater algae *Scenedesmus obliquus*, and the importance of humic acid in reducing toxicity. Nanotechnol. Environ. Eng. 9 (1), 85–98. https://doi.org/10.1007/s41204-023-00355-4.

Das, S., Thiagarajan, V., Chandrasekaran, N., Ravindran, B., Mukherjee, A., 2022. Nanoplastics enhance the toxic effects of titanium dioxide nanoparticle in freshwater algae *Scenedesmus obliquus*. Comp. Biochem. Physiol. C 256, 109305. https://doi.org/10.1016/j.cbpc.2022.109305.

Das, S., Giri, S., Jose, S.A., Pulimi, M., Anand, S., Chandrasekaran, N., Rai, P.K., Mukherjee, A., 2023a. Comparative toxicity assessment of individual, binary and ternary mixtures of SiO_2, Fe_3O_4, and ZnO nanoparticles in freshwater microalgae, *Scenedesmus obliquus*: exploring the role of dissolved ions. Comp. Biochem. Physiol. C 273, 109718. https://doi.org/10.1016/j.cbpc.2023.109718.

Das, S., Giri, S., Wadhwa, G., Pulimi, M., Anand, S., Chandrasekaran, N., Johari, S.A., Rai, P.K., Mukherjee, A., 2023b. Comparative ecotoxicity of graphene, functionalized multi-walled CNTs, and their mixture in freshwater microalgae, *Scenedesmus obliquus*: analyzing the role of oxidative stress. Environ. Sci. Pollut. Res. Int. 30 (27), 70246–70259. https://doi.org/10.1007/s11356-023-27367-6.

Dhall, A., Self, W., 2018. Cerium oxide nanoparticles: a brief review of their synthesis methods and biomedical applications. Antioxidants 7 (8), 97. https://doi.org/10.3390/antiox7080097.

Fu, L., Hamzeh, M., Dodard, S., Zhao, Y.H., Sunahara, G.I., 2015. Effects of TiO_2 nanoparticles on ROS production and growth inhibition using freshwater green algae pre-exposed to UV irradiation. Environ. Toxicol. Pharmacol. 39 (3), 1074–1080. https://doi.org/10.1016/j.etap.2015.03.015.

Gatou, M.-A., Syrrakou, A., Lagopati, N., Pavlatou, E.A., 2024. Photocatalytic TiO_2-based nanostructures as a promising material for diverse environmental applications: a review. Reactions 5 (1), 135–194. https://doi.org/10.3390/reactions5010007.

Ghariani, O., Elleuch, J., Gargouri, B., Fakhfakh, F., Bisio, C., Fendri, I., Guidotti, M., Abdelkafi, S., 2025. Toxicity potential assessment of silicon dioxide (SiO_2) and zinc oxide (ZnO) on green microalgae *Chlamydomonas* sp. strain GO1. Int. Microbiol. https://doi.org/10.1007/s10123-025-00635-w.

Ghazaei, F., Shariati, M., 2020. Effects of titanium nanoparticles on the photosynthesis, respiration, and physiological parameters in *Dunaliella salina* and *Dunaliella tertiolecta*. Protoplasma 257 (1), 75–88. https://doi.org/10.1007/s00709-019-01420-z.

Hua, J., Peijnenburg, W.J.G.M., Vijver, M.G., 2016. TiO_2 nanoparticles reduce the effects of ZnO nanoparticles and Zn ions on zebrafish embryos (Danio rerio). Nanoimpact 2, 45–53. https://doi.org/10.1016/j.impact.2016.06.005.

Huang, B., Wei, Z.B., Yang, L.Y., Pan, K., Miao, A.J., 2019. Combined toxicity of silver nanoparticles with hematite or plastic nanoparticles toward two freshwater algae. Environ. Sci. Technol. 53 (7), 3871–3879. https://doi.org/10.1021/acs.est.8b07001.

Huang, X.C., Huang, Y.C., Wang, D.L., Liu, M.X., Li, J., Chen, D., 2021. Cellular response of freshwater algae to halloysite nanotubes: alteration of oxidative stress and membrane function. Environ. Sci. Nano 8 (11), 3262–3272. https://doi.org/10.1039/d1en00531f.

Hund-Rinke, K., Sinram, T., Schlich, K., Nickel, C., Dickehut, H.P., Schmidt, M., Kuhnel, D., 2020. Attachment efficiency of nanomaterials to algae as an important criterion for ecotoxicity and grouping. Nanomaterials-Basel 10 (6). https://doi.org/10.3390/nano10061021.

Iswarya, V., Bhuvaneshwari, M., Alex, S.A., Iyer, S., Chaudhuri, G., Chandrasekaran, P. T., Bhalerao, G.M., Chakravarty, S., Raichur, A.M., Chandrasekaran, N., Mukherjee, A., 2015. Combined toxicity of two crystalline phases (anatase and

rutile) of titania nanoparticles towards freshwater microalgae: *Chlorella* sp. Aquat. Toxicol. 161, 154–169. https://doi.org/10.1016/j.aquatox.2015.02.006.
Joonas, E., Aruoja, V., Olli, K., Kahru, A., 2019. Environmental safety data on CuO and TiO_2 nanoparticles for multiple algal species in natural water: filling the data gaps for risk assessment. Sci. Total Environ. 647, 973–980. https://doi.org/10.1016/j.scitotenv.2018.07.446.
Keller, A.A., Slaveykova, V.I., 2025. Advances and challenges in the ecological risk assessment of engineered nanomaterials in aquatic ecosystems: a review. Sci. Total Environ. 1003, 180739. https://doi.org/10.1016/j.scitotenv.2025.180739.
Keller, A.A., Wang, H., Zhou, D., Lenihan, H.S., Cherr, G., Cardinale, B.J., Miller, R., Ji, Z., 2010. Stability and aggregation of metal oxide nanoparticles in natural aqueous matrices. Environ. Sci. Technol. 44 (6), 1962–1967. https://doi.org/10.1021/es902987d.
Ko, K.S., Koh, D.C., Kong, I.C., 2018. Toxicity evaluation of individual and mixtures of nanoparticles based on algal chlorophyll content and cell count. Materials 11 (1). https://doi.org/10.3390/ma11010121.
Kosak Nee Rohder, L.A., Brandt, T., Sigg, L., Behra, R., 2018. Uptake and effects of cerium(III) and cerium oxide nanoparticles to *Chlamydomonas reinhardtii*. Aquat. Toxicol. 197, 41–46. https://doi.org/10.1016/j.aquatox.2018.02.004.
Li, F., Liang, Z., Zheng, X., Zhao, W., Wu, M., Wang, Z., 2015. Toxicity of nano-TiO_2 on algae and the site of reactive oxygen species production. Aquat. Toxicol. 158, 1–13. https://doi.org/10.1016/j.aquatox.2014.10.014.
Li, M., Liu, W., Slaveykova, V.I., 2020. Effects of mixtures of engineered nanoparticles and metallic pollutants on aquatic organisms. Environments 7 (4). https://doi.org/10.3390/environments7040027.
Liu, Y., Wang, S., Wang, Z., Ye, N., Fang, H., Wang, D., 2018. TiO_2, SiO_2 and ZrO_2 nanoparticles synergistically provoke cellular oxidative damage in freshwater microalgae. Nanomaterials 8 (2). https://doi.org/10.3390/nano8020095.
Liu, W., Li, M., Li, W., Keller, A.A., Slaveykova, V.I., 2022. Metabolic alterations in alga Chlamydomonas reinhardtii exposed to nTiO_2 materials. Environ. Sci. Nano 9 (8), 2922–2938. https://doi.org/10.1039/d2en00260d.
Liu, S., Han, J., Ma, X., Zhu, X., Qu, H., Xin, G., Huang, X., 2024. Repeated release of cerium oxide nanoparticles altered algal responses: growth, photosynthesis, and photosynthetic gene expression. Eco-Environ. Health 3 (3), 290–299. https://doi.org/10.1016/j.eehl.2024.04.002.
Luo, M., Qi, X., Ren, T., Huang, Y., Keller, A.A., Wang, H., Wu, B., Jin, H., Li, F., 2017. Heteroaggregation of CeO_2 and TiO_2 engineered nanoparticles in the aqueous phase: application of turbiscan stability index and fluorescence excitation-emission matrix (EEM) spectra. Colloids Surf. A Physicochem. Eng. Asp. 533, 9–19. https://doi.org/10.1016/j.colsurfa.2017.08.014.
Machado, M.D., Soares, E.V., 2024. Features of the microalga *Raphidocelis subcapitata*: physiology and applications. Appl. Microbiol. Biotechnol. 108 (1), 219. https://doi.org/10.1007/s00253-024-13038-0.
Mackevica, A., Hendriks, L., Meili-Borovinskaya, O., Baun, A., Skjolding, L.M., 2023. Effect of exposure concentration and growth conditions on the association of cerium oxide nanoparticles with green algae. Nanomaterials 13 (17). https://doi.org/10.3390/nano13172468.
Mahaye, N., Musee, N., 2023. Evaluation of apical and molecular effects of algae *Pseudokirchneriella subcapitata* to cerium oxide nanoparticles. Toxics 11 (3). https://doi.org/10.3390/toxics11030283.
Manier, N., Bado-Nilles, A., Delalain, P., Aguerre-Chariol, O., Pandard, P., 2013. Ecotoxicity of non-aged and aged CeO_2 nanomaterials towards freshwater microalgae. Environ. Pollut. 180, 63–70. https://doi.org/10.1016/j.envpol.2013.04.040.
Martinez, D.S.T., Ellis, L.J.A., Da Silva, G.H., Petry, R., Medeiros, A.M.Z., Davoudi, H.H., Papadiamantis, A.G., Fazzio, A., Afantitis, A., Melagraki, G., Lynch, I., 2022. *Daphnia magna* and mixture toxicity with nanomaterials - current status and perspectives in data-driven risk prediction. Nano Today 43. https://doi.org/10.1016/j.nantod.2022.101430.
Mohajeri, M., Momenai, R., Karami-Mohajeri, S., Ohadi, M., Raeisi Estabragh, M.A., 2025. Cerium oxide nanoparticles, physical and chemical properties, applications and toxicological implications: a review. Results Chem. 15, 102302. https://doi.org/10.1016/j.rechem.2025.102302.
Mosleminejad, N., Ghasemi, Z., Johari, S.A., 2024. Ionic and nanoparticulate silver alleviate the toxicity of inorganic mercury in marine microalga *Chaetoceros muelleri*. Environ. Sci. Pollut. Res. Int. 31 (13), 19206–19225. https://doi.org/10.1007/s11356-024-32120-8.
Musial, J., Krakowiak, R., Mlynarczyk, D.T., Goslinski, T., Stanisz, B.J., 2020. Titanium dioxide nanoparticles in food and personal care products-what do we know about their safety? Nanomaterials 10 (6). https://doi.org/10.3390/nano10061110.
Neale, P.A., Jämting, Å.K., O'Malley, E., Herrmann, J., Escher, B.I., 2015. Behaviour of titanium dioxide and zinc oxide nanoparticles in the presence of wastewater-derived organic matter and implications for algal toxicity. Environ. Sci. Nano 2 (1), 86–93. https://doi.org/10.1039/c4en00161c.
OECD, 2011. Test No. 201: Freshwater Alga and Cyanobacteria, Growth Inhibition Test, OECD Publishing, Paris, OECD Guidelines for the Testing of Chemicals, Section 2: Effects on Biotic Systems. OECD Publishing, New York, NY, USA.
Ozkaleli, M., Erdem, A., 2018. Biotoxicity of TiO_2 nanoparticles on *Raphidocelis subcapitata* microalgae exemplified by membrane deformation. Int. J. Environ. Res. Public Health 15 (3). https://doi.org/10.3390/ijerph15030416.
Pace, H.E., Rogers, N.J., Jarolimek, C., Coleman, V.A., Higgins, C.P., Ranville, J.F., 2011. Determining transport efficiency for the purpose of counting and sizing nanoparticles via single particle inductively coupled plasma mass spectrometry. Anal. Chem. 83 (24), 9361–9369. https://doi.org/10.1021/ac201952t.
Pansambal, S., Oza, R., Borgave, S., Chauhan, A., Bardapurkar, P., Vyas, S., Ghotekar, S., 2022. Bioengineered cerium oxide (CeO_2) nanoparticles and their diverse applications: a review. Appl. Nanosci. 13 (9), 6067–6092. https://doi.org/10.1007/s13204-022-02574-8.
Pecoraro, R., Scalisi, E.M., Indelicato, S., Contino, M., Coco, G., Stancanelli, I., Capparucci, F., Fiorenza, R., Brundo, M.V., 2023. Toxicity of titanium dioxide-cerium oxide nanocomposites to zebrafish embryos: a preliminary evaluation. Toxics 11 (12). https://doi.org/10.3390/toxics11120994.
Pikula, K., Johari, S.A., Santos-Oliveira, R., Golokhvast, K., 2022. Individual and binary mixture toxicity of five nanoparticles in marine microalga *Heterosigma akashiwo*. Int. J. Mol. Sci. 23 (2). https://doi.org/10.3390/ijms23020990.
Pulido-Reyes, G., Briffa, S.M., Hurtado-Gallego, J., Yudina, T., Leganés, F., Puntes, V., Valsami-Jones, E., Rosal, R., Fernández-Piñas, F., 2019. Internalization and toxicological mechanisms of uncoated and PVP-coated cerium oxide nanoparticles in the freshwater alga. Environ. Sci. Nano 6 (6), 1959–1972. https://doi.org/10.1039/c9en00363k.
Rana, S., Kumar, A., 2023a. Ecotoxicity of a mixture of nanoparticles on algal species *Scendesmus obliquus* in OECD growth media, wastewater, and pond water. Ecotoxicology 32 (10), 1257–1271. https://doi.org/10.1007/s10646-023-02718-8.
Rana, S., Kumar, A., 2023b. Effect of long-term exposure of mixture of ZnO and CuO nanoparticles on *Scenedesmus obliquus*. Ecotoxicology 32 (10), 1233–1246. https://doi.org/10.1007/s10646-023-02710-2.
Rasmussen, K., Jan Mast, P.-J.D.T., Eveline Verleysen, N.W., Steen, F.V., Pizzolon, J.C., Temmerman, L.D., Doren, E.V., Jensen, K.A., Birkedal, R., Levin, M., Nielsen, S.H., Koponen, I.K., Clausen, P.A., Kofoed-Sørensen, V., Kembouche, Y., Thieriet, N., Spalla, O., Guiot, C., Rousset, D., Witschger, O., Bau, S., Bianchi, B., Motzkus, C., Shivachev, B., Dimowa, L., Nikolova, R., Nihtianova, D., Tarassov, M., Petrov, O., Bakardjieva, S., Gilliland, D., Pianella, F., Ceccone, G., Spampinato, V., Cotogno, G., Gibson, N., Gaillard, C., Mech, A., 2014. Titanium Dioxide, NM-100, NM-101, NM-102, NM-103, NM-104, NM-105: Characterisation and Physico-Chemical Properties JRC Repository: NM-series of Representative Manufactured Nanomaterials. https://doi.org/10.2788/79554.
Rosario, F., Costa, C., Lopes, C.B., Estrada, A.C., Tavares, D.S., Pereira, E., Teixeira, J.P., Reis, A.T., 2022. In vitro hepatotoxic and neurotoxic effects of titanium and cerium dioxide nanoparticles, arsenic and mercury co-exposure. Int. J. Mol. Sci. 23 (5). https://doi.org/10.3390/ijms23052737.
Roy, B., Suresh, P.K., Chandrasekaran, N., Mukherjee, A., 2021. Antibiotic tetracycline enhanced the toxic potential of photo catalytically active P25 titanium dioxide nanoparticles towards freshwater algae *Scenedesmus obliquus*. Chemosphere 267, 128923. https://doi.org/10.1016/j.chemosphere.2020.128923.
Sanchez-Garcia, L., Bolea, E., Laborda, F., Cubel, C., Ferrer, P., Gianolio, D., da Silva, I., Castillo, J.R., 2016. Size determination and quantification of engineered cerium oxide nanoparticles by flow field-flow fractionation coupled to inductively coupled plasma mass spectrometry. J. Chromatogr. A 1438, 205–215. https://doi.org/10.1016/j.chroma.2016.02.036.
Santos, J.P., Li, W., Keller, A.A., Slaveykova, V.I., 2024. Mercury species induce metabolic reprogramming in freshwater diatom *Cyclotella meneghiniana*. J. Hazard. Mater. 465, 133245. https://doi.org/10.1016/j.jhazmat.2023.133245.
Schiavo, S., Oliviero, M., Philippe, A., Manzo, S., 2018. Nanoparticles based sunscreens provoke adverse effects on marine microalgae *Dunaliella tertiolecta*. Environ. Sci. Nano 5 (12), 3011–3022. https://doi.org/10.1039/c8en01182f.
Singh, C., Steffi, F., Ceccone, G., Gibson, N., Jensen, A., Levin, M., Goenaga-Infante, H., David, C., Rasmussen, K., 2014. Cerium dioxide, NM-211, NM-212, NM-213. Characterisation and Test Item Preparation. JRC Science and Policy Reports. https://doi.org/10.2788/80203.
Suárez-Oubiña, C., Herbello-Hermelo, P., Bermejo-Barrera, P., Moreda-Piñeiro, A., 2022. Exploiting dynamic reaction cell technology for removal of spectral interferences in the assessment of ag, cu, Ti, and Zn by inductively coupled plasma mass spectrometry. Spectrochim. Acta B At. Spectrosc. 187. https://doi.org/10.1016/j.sab.2021.106330.
Suarez-Oubina, C., Herbello-Hermelo, P., Mallo, N., Vazquez, M., Cabaleiro, S., Pinheiro, I., Rodriguez-Lorenzo, L., Espina, B., Bermejo-Barrera, P., Moreda-Pineiro, A., 2023. Single-cell ICP-MS for studying the association of inorganic nanoparticles with cell lines derived from aquaculture species. Anal. Bioanal. Chem. 415 (17), 3399–3413. https://doi.org/10.1007/s00216-023-04723-6.
Vilela, P., Jácome, G., Moya, W., Ifaei, P., Heo, S., Yoo, C., 2023. A brief insight into the toxicity conundrum: modeling, measuring, monitoring and evaluating ecotoxicity for water quality towards environmental sustainability. Sustainability 15 (11), 8881. https://doi.org/10.3390/su15118881.
von Moos, N., Slaveykova, V.I., 2014. Oxidative stress induced by inorganic nanoparticles in bacteria and aquatic microalgae – state of the art and knowledge gaps. Nanotoxicology 8 (6), 605–630. https://doi.org/10.3109/17435390.2013.809810.
Wang, Z., Jin, S., Zhang, F., Wang, D., 2020. Combined toxicity of TiO_2 Nanospherical particles and TiO_2 nanotubes to two microalgae with different morphology. Nanomaterials 10 (12). https://doi.org/10.3390/nano10122559.
Wang, D.X., Mao, W.F., Zhao, L.H., Meng, D., Wu, T.F., 2024a. Effects of aggregation and settling of photoactive TiO_2 nanoparticles on *Microcystis aeruginosa* and extracellular matters release. Algal Res. 82. https://doi.org/10.1016/j.algal.2024.103626.
Wang, D., Pan, Q., Yang, J., Gong, S., Liu, X., Fu, Y., 2024b. Effects of mixtures of engineered nanoparticles and Cocontaminants on anaerobic digestion. Environ. Sci. Technol. 58 (6), 2598–2614. https://doi.org/10.1021/acs.est.3c09239.
Wu, D., Zhang, J.J., Du, W.C., Yin, Y., Guo, H.Y., 2022. Toxicity mechanism of cerium oxide nanoparticles on cyanobacteria *Microcystis aeruginosa* and their ecological risks. Environ. Sci. Pollut. Res. 29 (23), 34010–34018. https://doi.org/10.1007/s11356-021-18090-1.
Xia, B., Chen, B., Sun, X., Qu, K., Ma, F., Du, M., 2015. Interaction of TiO_2 nanoparticles with the marine microalga *Nitzschia closterium*: growth inhibition, oxidative stress

and internalization. Sci. Total Environ. 508, 525–533. https://doi.org/10.1016/j.scitotenv.2014.11.066.

Ye, N., Wang, Z., Wang, S., Peijnenburg, W., 2018. Toxicity of mixtures of zinc oxide and graphene oxide nanoparticles to aquatic organisms of different trophic level: particles outperform dissolved ions. Nanotoxicology 12 (5), 423–438. https://doi.org/10.1080/17435390.2018.1458342.

Yu, R., Wu, J., Liu, M., Chen, L., Zhu, G., Lu, H., 2016a. Physiological and transcriptional responses of *Nitrosomonas europaea* to TiO^2 and ZnO nanoparticles and their mixtures. Environ. Sci. Pollut. Res. Int. 23 (13), 13023–13034. https://doi.org/10.1007/s11356-016-6469-8.

Yu, R., Wu, J., Liu, M., Zhu, G., Chen, L., Chang, Y., Lu, H., 2016b. Toxicity of binary mixtures of metal oxide nanoparticles to *Nitrosomonas europaea*. Chemosphere 153, 187–197. https://doi.org/10.1016/j.chemosphere.2016.03.065.

Zhang, F., Wang, Z., Peijnenburg, W., Vijver, M.G., 2022. Review and prospects on the Ecotoxicity of mixtures of nanoparticles and hybrid nanomaterials. Environ. Sci. Technol. 56 (22), 15238–15250. https://doi.org/10.1021/acs.est.2c03333.